Journal of Crystal Growth 324 (2011) 259–262

Contents lists available at ScienceDirect

Journal of Crystal Growth

journal homepage: www.elsevier.com/locate/jcrysgro

Optical microcavities fabricated by DBR overgrowth of pyramidal-shaped GaAs mesas

D. Rülke *, M. Karl, D.Z. Hu, D.M. Schaadt, H. Kalt, M. Hetterich

Institut für Angewandte Physik and DFG Center for Functional Nanostructures (CFN), Karlsruhe Institute of Technology (KIT), Wolfgang-Gaede-Straße 1, D-76131 Karlsruhe, Germany

ARTICLE INFO

Article history:
Received 22 October 2010
Received in revised form
21 March 2011
Accepted 22 March 2011
Communicated by K.W. Benz
Available online 30 March 2011

Keywords:
A1. Optical microscopy
A1. Etching
A1. Nanostructures
A3. Molecular beam epitaxy
B1. Arsenates
B2. Semiconducting III–V materials

ABSTRACT

Optical cavities have been fabricated by overgrowth of truncated GaAs pyramids with a distributed Bragg reflector. The success of this overgrowth depends strongly on the crystallographic orientation of the pyramid facets and shows best results for {1 1 4} A facets. In order to fabricate mesas with precisely such facets, a wet-chemical etching process including several selective etching steps has been established. To determine the optical properties of these resonators, InAs quantum dots have been used as an internal broad-band light source. The quality factors for optical modes have been determined to range up to 8000 and show a dependency on cavity width.

The interaction of quantum dots (QDs) with the electric field of an optical cavity mode has been of high interest, motivated by possible applications in quantum information processing and quantum communication [1–3]. It has been demonstrated that the efficiency as well as the detection probability of the quantum dot emission can be drastically enhanced if a discrete excitonic QD state is brought into resonance with an optical mode [4,5]. In combination with the narrow linewidth of QD states, this effect encouraged the fabrication of high-efficiency single photon sources [6,7]. Furthermore, a strong coupling of single excitonic quantum dot states with optical cavity modes [8] has been achieved, which might be the first step towards a coherent coupling of spatially separated quantum dots via the electric field of a cavity mode [1].

The prerequisite to observe any of these cavity quantum electrodynamic effects is to design optical resonators with high quality factor (Q) and low mode volume that additionally allow to place quantum dots at the antinode of optical modes. Besides photonic crystal structures, micropillars which consist of a cylindric λ-cavity sandwiched between two distributed Bragg reflectors (DBRs) have been investigated intensely in this context, especially in the combination of In(Ga)As QDs within a GaAs cavity and an Al(Ga)As/GaAs DBR (see e.g. [9–11] and references therein). The efficiency to couple light from the internal source into a high-Q mode is thereby limited due to a high density of leaky modes, that appear through losses and defect-related background absorption at the surface of the cavity, where the light is confined via total internal reflection [10,11]. This argument is confirmed by a strong decrease of the quality for pillar diameters below 4 μm, when the antinode of the mode gets closer to the GaAs surface.

In order to minimize these losses and to reduce the often undesirable leaky modes found e.g. in pillar resonators, we develop GaAs cavities completely covered with AlAs/GaAs DBRs, such that the light would be confined exclusively by the latter. To this end, the perpendicular edges of the conventional pillar cavity had to be flatted, since it seemed very unlikely to grow a high-quality DBR perpendicular and parallel to the substrate orientation at the same time. In addition, one should take into account, that the stop band position of a Bragg mirror strongly depends on the incident angle of incoming light. For these reasons, we decided to establish a fabrication process that ends up in the overgrowth of truncated pyramids with gently sloped facets [12,13].

The design of the cavities was inspired by our former observation that during overgrowth with an AlAs/GaAs heterostructure smooth {1 1 4} A facets arose on mesas offering only edges within the {1 1 4} A planes (Fig. 1). Whereas on the mesa facets, the

* Corresponding author.
E-mail address: daniel.ruelke@kit.edu (D. Rülke).

0022-0248/$ - see front matter © 2011 Elsevier B.V. All rights reserved.
doi:10.1016/j.jcrysgro.2011.03.041

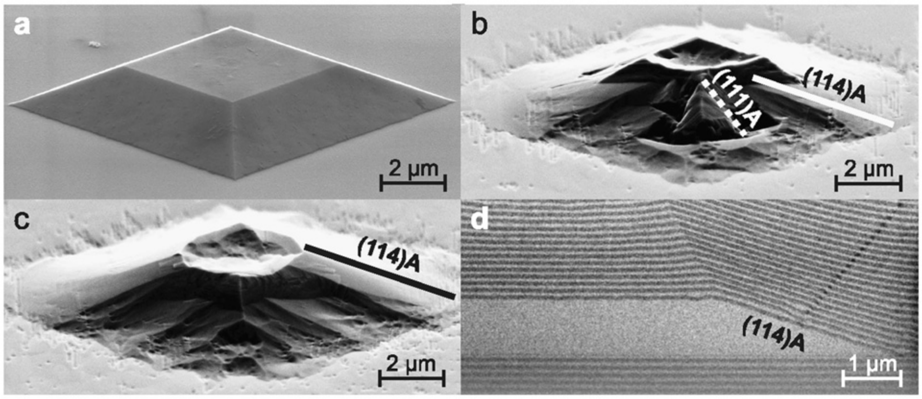

Fig. 1. During overgrowth of a truncated pyramid with {2 1 0} facets (a) steps appear roughly oriented to {1 1 1} A (b) and {1 1 4} A planes (b, c). A new smooth {1 1 4} A facet was created on the edge of the truncated pyramid. Its orientation can clearly be identified by a focussed ion beam cut along the diagonal of the truncated pyramid (d).

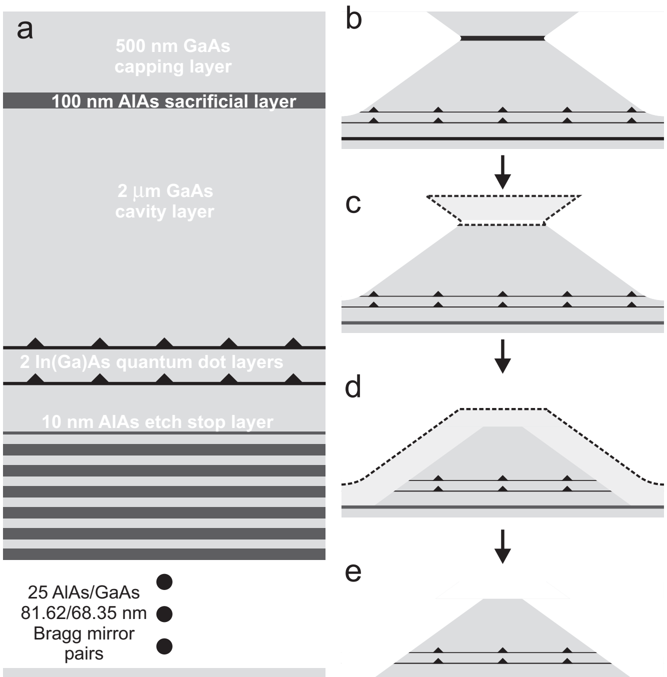

Fig. 2. After etching of the initial layer structure (a) with a phosphoric acid solution (b) and removing of the AlAs sacrificial layer, a truncated pyramid is obtained (c). This pyramid is etched down to the AlAs etch stop layer with a citric acid solution (d) and after the stop layer has been removed, the lower DBR is uncovered (e).

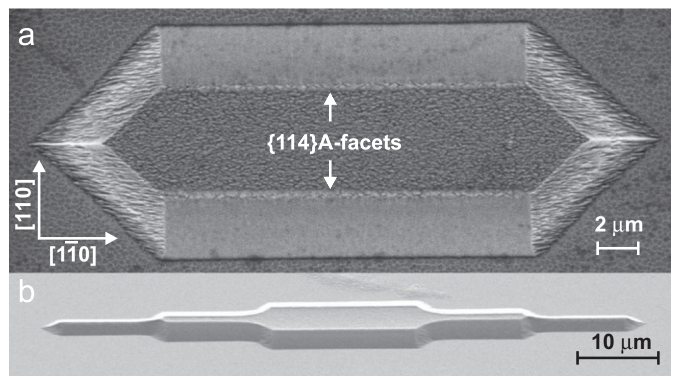

Fig. 3. Scanning electron micrographs of two cavities obtained by different masks, top (a) and side view (b), respectively. The anisotropically etched {1 1 4} A facets are much smoother compared to isotropically etched facets.

overgrowth produced step-like structures roughly oriented to the {1 1 1} A and {1 1 4} A planes, that could be due to formation of low energy surfaces and different adatom mobilities on the A and B planes. To overgrow in a controlled manner, the cavity surface was therefore prepared to provide as much of the {1 1 4} A facets as possible. The height of the cavity was chosen to be about 1.2 μm before overgrowth. This ensured that around the design wavelength of the DBR the spectral distance between two subsequent Fabry–Pérot modes was smaller than the width of the stop band. In other words, at least one of these Fabry–Pérot modes should have its spectral position inside the stop band even if the exact value of the height was unknown.

The initial layer structure (Fig. 2a) was grown by molecular-beam epitaxy on a (0 0 1)-oriented Zn-doped GaAs substrate. First, a DBR consisting of 25 pairs of alternating 81.62 nm AlAs and 68.35 nm GaAs layers was grown with a 10 nm AlAs etch stop layer on top. Then, a 2 μm GaAs cavity with two InAs QD layers embedded 400 and 600 nm above the DBR were grown, followed by a 100 nm AlAs sacrificial and a 500 nm GaAs capping layer. The density of the QDs per layer was in the range of 10^9-10^{10} cm^{-2} and their mean emission wavelength about 950 nm at low temperature.

After an e-beam lithography step, at which the mask pattern had been oriented just as the surfaces of the mesas shown in Fig. 3, the initial rough exposing of the {1 1 4} A planes on the sidewalls of the mesas was performed by a wet-chemical etching process (Fig. 2b), that allows to adjust the angle between the substrate and the sidewalls from 25° to 65° by varying the hydrogen peroxide content of an 1:*x*:8 H_3PO_4:H_2O_2:H_2O etching solution [12,14]. This variation of the ingredients changes the etching rates in the AlAs sacrificial layer and the GaAs as well as their ratio, leading to a more or less pronounced undercut on the level of the sacrificial layer.

Right before the GaAs in the surroundings of the mask pattern was etched down to the DBR, the etching was interrupted and the AlAs sacrificial layer was removed selectively with an 1:0.1:8 H_3PO_4:H_2O_2:H_2O etching solution (Fig. 2c). The remaining GaAs structure was etched selectively with citric acid (CA) (100 g $C_6H_8O_7$:100 ml H_2O) and H_2O_2 with a ratio of 5:1, CA:H_2O_2 [15] until the cavity height was ~1.2 μm (Fig. 2d). During this part of the etching procedure, the surrounding GaAs was completely etched down to the AlAs etch stop layer and after removing the AlAs layer, different kinds of truncated pyramids with {1 1 4} A facets on a flat DBR surface were obtained (Fig. 2e).

The mentioned precise uncovering of the bottom DBR was necessary for two reasons: On the one hand, no GaAs, possibly acting as a waveguide between the two DBRs, should be left on

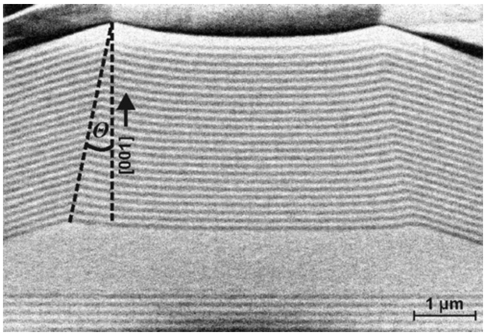

Fig. 4. Cross-section of an overgrown cavity received by a focussed ion beam cut. The vertex of two adjacent facets is propagating with an angle Θ during overgrowth.

the top of the bottom DBR. On the other hand, it should be avoided that the etchant penetrates the DBR and produces steps due to different etching rates in AlAs and GaAs, unavoidably leading to worse conditions for a subsequent overgrowth. The mesa facets were perfectly aligned to the crystallographic planes due to the anisotropic etching behavior of citric acid and were much smoother than facets which are usually achieved by isotropic etching (Fig. 3). Finally, the pre-patterned substrate was directly overgrown with 20 AlAs/GaAs DBR pairs.

Cutting through an overgrown cavity (Fig. 4) reveals, that the area of the top DBR was successively reduced by the edges of the opposing tilted DBR stacks during overgrowth. This effect was geometrically explained in [16] and depends on the facet orientation and the growth rates on the facets. The propagation angle Θ of the vertex of two adjacent facets can be described correspondingly by the following equation:

$$\frac{r_1}{r_2} = \frac{\cos(\alpha_1+\Theta)}{\cos(\alpha_2-\Theta)}, \qquad (1)$$

where r_1, r_2 are the growth rates and α_1, α_2 are the angles between the facet normals and the [0 0 1] direction of the two facets.

Using the measured propagation angle $\Theta \sim 8^\circ$, the ratio $r_{[1\ 1\ 4]A}/r_{[0\ 0\ 1]}$ is determined to be 1 within the uncertainness of the scanning electron microscope image analysis. During overgrowth, the two opposing propagating vertices decrease the width of the DBR top surface by about 1 μm compared to the initial width of the cavity top surface. Additionally, the top DBR showed a small curvature near the edges. This indicates a slightly enhanced growth rate at the convex vertices of vicinal facets which can be observed from the very beginning of the 15 nm buffer layer right below the top DBR (Fig. 4). This effect becomes stronger for acute vertices and suggests the use of flat facets. For these reasons, it was necessary to start overgrowth with cavity surfaces wider than 4 μm, since the DBR along the [0 0 1] direction would not grow continuously until the end otherwise. Nevertheless, the DBR on the {1 1 4} A facets and, if the plateau on the mesa was wide enough, the DBR on the (0 0 1) top surface could be grown with reasonable quality.

In order to analyze their optical properties, the samples were mounted in the cryostat of a confocal micro-photoluminescence (μ-PL) setup. After excitation slightly below the GaAs band-gap or into the InAs wetting layer with a tunable titanium:sapphire laser, the light was dispersed by a 0.85 m double-spectrometer equipped with a silicon charge-coupled device for detection. The system had a spectral resolution of ~ 0.05 nm and a spatial resolution of ~ 1 μm.

In the μ-PL spectra of various mesas, several sharp peaks were identified as optical modes through the thermal shift of their resonance wavelength [12]. It was also observed that generally a fundamental mode with the lowest photon energy is followed by resonances with higher energies. This behavior can be explained by the presence of higher-order states due to a lateral confinement by the tilted Bragg stacks on the mesa facets in addition to the vertical confinement by the parallel Bragg stacks underneath and above the cavity. It might be a hint for low-loss lateral confinement, that the quality of higher-order confined modes does not significantly decrease compared to the fundamental mode. The Q factors of the sharpest observed resonances were determined to usually range from 1000 up to 8000 (Fig. 5) for each of the different shaped and sized overgrown structures on this sample (in comparison with $Q \sim 700$ for non-overgrown pyramids [13]). For a comparable number of DBR stacks above (20) and below (24) the cavity and a diameter of 4 μm only a slightly better Q factor of 9300 has been reported for micropillar cavities [9]. In comparison with resonances from non-overgrown pyramidal cavities [12,13], the background emission due to low-Q 'leaky' modes appears to be strongly reduced, but still varies for different cavities (compare background emission in Fig. 5a and b).

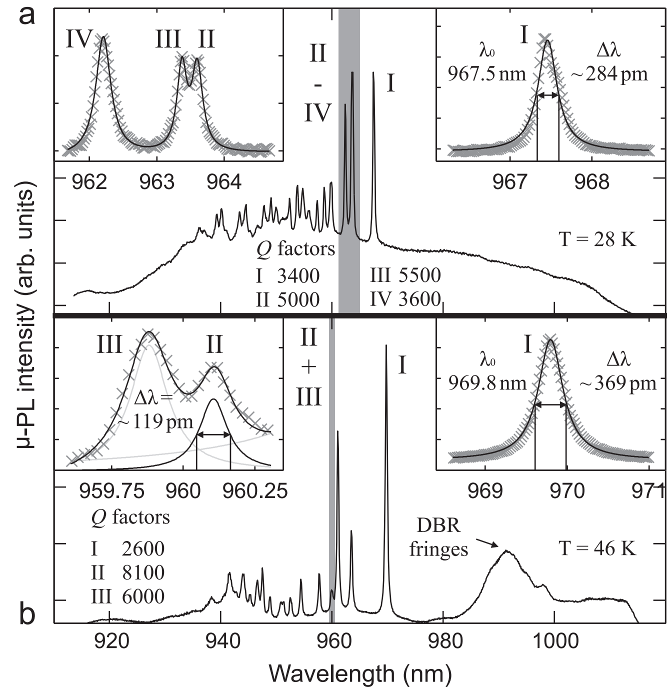

Fig. 5. Spectra of overgrown cavities comparable to those which can be seen uncovered in Fig. 3(a) and (b), respectively. Despite the different shapes of the cavities, the features in both spectra are quite similar, whereas the QD background emission seems to be suppressed in (b) more strongly. The insets show fits of Lorentzian distributions to the fundamental modes and some elected modes highlighted in the spectra. Center emission wavelength of QDs is about 950 nm at 4 K.

The quality of optical modes exhibit strong correlation to the visually observable quality of the top DBR. The Q factor of optical modes stays almost constant for different shapes and sizes of {1 1 4} A-faceted mesas, if the top surface of the cavity is wider than 4 μm. Keeping in mind the decreasing size of the top DBR, this is consistent with results from FDTD simulations that never showed any clear optical modes for rotation-symmetric non-truncated overgrown cavities. For {0 k l}-facets no optical modes could be observed experimentally.

In conclusion, we have proved the DBR overgrowth of truncated GaAs pyramids to be feasible for the fabrication of high-Q optical resonators with a reduced influence of leaky modes. The overgrowth quality mainly depends on the crystallographic orientation of the pyramid facets. Therefore, for overgrown truncated pyramids with {1 1 4} A facets optical modes with quality factors up to 8000 were observed, if the cavity was wider than $\sim 4\,\mu m$, whereas no defined modes could be observed for arbitrarily oriented facets.

This work has been performed within project A2 of the DFG Research Center for Functional Nanostructures (CFN). It has been further supported by a grant from the Ministry of Science, Research and the Arts of Baden-Württemberg (Az: 7713.14-300). We further acknowledge support by the Karlsruhe School of Optics and Photonics (KSOP).

References

[1] A. Imamoğlu, D.D. Awschalom, G. Burkard, D.P. DiVincenzo, D. Loss, M. Sherwin, A. Small, Quantum information processing using quantum dot spins and cavity QED, Phys. Rev. Lett. 83 (20) (1999) 4204–4207.
[2] X.-Q. Li, Y. Yan, Quantum computation with coupled quantum dots embedded in optical microcavities, Phys. Rev. B 65 (20) (2002) 205301.
[3] A. Kiraz, M. Atatüre, A. Imamoğlu, Quantum-dot single-photon sources: prospects for applications in linear optics quantum-information processing, Phys. Rev. A 69 (3) (2004) 032305.
[4] J.-M. Gerard, B. Gayral, Strong purcell effect for InAs quantum boxes in three-dimensional solid-state microcavities, J. Lightwave Technol. 17 (11) (1999) 2089–2095.
[5] D. Englund, D. Fattal, E. Waks, G. Solomon, B. Zhang, T. Nakaoka, Y. Arakawa, Y. Yamamoto, J. Vučković, Controlling the spontaneous emission rate of single quantum dots in a two-dimensional photonic crystal, Phys. Rev. Lett. 95 (1) (2005) 013904.
[6] P. Michler, A. Kiraz, C. Becher, W.V. Schoenfeld, P.M. Petroff, L. Zhang, E. Hu, A. Imamoglu, A quantum dot single-photon turnstile device, Science 290 (5500) (2000) 2282–2285.
[7] T. Heindel, C. Schneider, M. Lermer, S.H. Kwon, T. Braun, S. Reitzenstein, S. Höfling, M. Kamp, A. Forchel, Electrically driven quantum dot-micropillar single photon source with 34% overall efficiency, Appl. Phys. Lett. 96 (1) (2010) 011107.
[8] G. Khitrova, H.M. Gibbs, M. Kira, S.W. Koch, A. Scherer, Vacuum rabi splitting in semiconductors, Nat. Phys. 2 (2) (2006) 81–90.
[9] S. Reitzenstein, A. Forchel, Quantum dot micropillars, J. Phys. D: Appl. Phys. 43 (3) (2010) 033001.
[10] S. Reitzenstein, C. Hofmann, A. Gorbunov, M. Strauss, S.H. Kwon, C. Schneider, A. Löffler, S. Höfling, M. Kamp, A. Forchel, AlAs/GaAs micropillar cavities with quality factors exceeding 150.000, Appl. Phys. Lett. 90 (25) (2007) 251109.
[11] M. Karl, B. Kettner, S. Burger, F. Schmidt, H. Kalt, M. Hetterich, Dependencies of micro-pillar cavity quality factors calculated with finite element methods, Opt. Express 17 (2) (2009) 1144–1158.
[12] F.M. Weber, M. Karl, J. Lupaca-Schomber, W. Löffler, S. Li, T. Passow, J. Hawecker, D. Gerthsen, H. Kalt, M. Hetterich, Optical modes in pyramidal GaAs microcavities, Appl. Phys. Lett. 90 (16) (2007) 161104.
[13] M. Karl, T. Beck, S. Li, H. Kalt, M. Hetterich, Q-factor and density of optical modes in pyramidal and cone-shaped GaAs microcavities, Appl. Phys. Lett. 92 (23) (2008) 231105.
[14] V. Cambel, D. Gregušová, R. Kúdela, Formation of GaAs three-dimensional objects using AlAs "facet-forming" sacrificial layer and H_3PO_4, H_2O_2, H_2O based solution, J. Appl. Phys. 94 (7) (2003) 4643–4648.
[15] G.C. DeSalvo, W.F. Tseng, J. Comas, Etch rates and selectivities of citric acid/hydrogen peroxide on GaAs, $Al_{0.3}Ga_{0.7}As$, $In_{0.2}Ga_{0.8}As$, $In_{0.53}Ga_{0.47}As$, $In_{0.52}Al_{0.48}As$, and InP, J. Electrochem. Soc. 139 (3) (1992) 831.
[16] J.S. Smith, P.L. Derry, S. Margalit, A. Yariv, High quality molecular beam epitaxial growth on patterned GaAs substrates, Appl. Phys. Lett. 47 (7) (1985) 712–715.